Highly Sensitive Narrowband Si Photodetector With Peak Response at Around 1060 nm

Li Wang, Hehao Luo, Huanhuan Zuo, Jiqing Tao, Yongqiang Yu, Xiaoping Yang, Molin Wang, Jigang Hu, Chao Xie, Di Wu, and Linbao Luo, *Senior Member, IEEE*

***Abstract*— Photodetection at a wavelength of about 1060 nm is very important for applications including medical imaging, optical communication, and light detection and ranging. In this article, a self-powered near-infrared light detector with a narrowband at around 1060 nm is realized based on a simple Si Schottky structure, in which the Ohmic and Schottky electrodes are configured on the front and rear surfaces of the Si substrate, respectively. The as-assembled device exhibits a tunable peak response near 1060 nm with a full width at half maximum of 107 nm, which could be due to the combined effect of the narrow photo-current generation and the self-filtering effect of the silicon substrate. At zero bias, a specific detectivity of $\sim 1 \times 10^{11}$ Jones and linear dynamic range about 101 dB are achieved, in spite of the weak absorption of Si at this wavelength. The external quantum efficiency can be improved to 135% under a low bias of −1 V, indicating the existence of gain mechanism during photodetection. Finally, it is also found that the as-assembled near-infrared device shows excellent antiinterference capability during the photodetection process. These results corroborate that the present Si photodetector may find promising application in future near-infrared optoelectronic devices and systems.**

***Index Terms*— External quantum efficiency (EQE), linear dynamic range (LDR), narrowband photodetector, near-infrared light, silicon.**

I. Introduction

THE specific wavelength window at around 1060 nm (typically 1000–1100 nm) is vitally important in many fields such as medical imaging, optical communication system, and light detection and ranging [1]. It has been considered very important for ophthalmic optical coherence tomography imaging as the water absorption and scattering effect in the eyes was balanced in this band [2]. What is more, the current state-of-the-art technology of high repetition rate and power lasers propels the utilization of near-infrared 1064 nm wavelength to construct the optical data link, which exhibits larger data transfer rate and reduced transmission power compared with traditional microwaves [3].

As a core component of some complicated infrared systems, the photodetector often suffers from poor detection limit, which is usually not determined by the noise coming from device itself, but by background disturbance, in that the light incident on device is a combination of object information and background radiation [4]. The development of a photodetector with peak response to target wavelength is an effective solution to boost the immunity of an infrared system to background interference. To date, very few studies about the narrowband 1060 nm photodetector has been reported, except for some reliable narrowband devices at other wavelengths which are based on the following geometies: broadband photodiodes combined with optical filters [5], [6], bulk heterojunction based on the charge collection narrowing mechanism [7], [8], nanowire arrays [9], [10], narrowband absorption active layer [11]–[14], and periodic metallic hole/slit structures on semiconductor [15], [16]. However, it is undeniable that the majority of the above narrowband devices are usually complex in architectures, or unstable for the usage of organic photoactive layers [17]. Moreover, external power supply is needed during operation, which restricts the application of these devices in optic-electronic integration requiring component miniaturization. In this article, a self-powered narrowband photodetector with peak response near 1060 nm was fabricated based on a simple Si Schottky structure, which can effectively improve the noise immunity of infrared system in detecting a target signal of 1060 nm.

II. Experimental Details

A. Device Fabrication

The narrowband Si Schottky-junction photodetector was fabricated on a commercially available n-type (100) Si wafer substrate (resistivity: 1–10 Ωcm, single side polished). After the removal of the oxidation layer on Si by immersing the substrate into a buffered oxide etch (BOE) solution (HF: NH_4F:H_2O = 3 mL:6 g:10 mL) for 3 min, a rectangle window (0.2 cm × 0.25 cm) was first defined on the polished surface of Si substrate using an insulation tape. Then different metal Schottky films of 50 nm thickness were deposited onto the substrate, including Au, Ag, and Al. For comparison, graphene film has also been transferred onto the substrate as the Schottky contact. Meanwhile Ohmic contact was obtained

Manuscript received May 8, 2020; revised May 31, 2020; accepted June 4, 2020. Date of publication June 22, 2020; date of current version July 23, 2020. This work was supported in part by the Natural Science Foundation of China under Grant 61575059 and Grant 61675062, in part by Fundamental Research Funds for the Central Universities under Grant JZ2018HGPB0275, Grant JZ2018HGTA0220, and Grant JZ2018HGXC000, and in part by the National College Students' Innovation and Entrepreneurship Training Program under Grant 201710359060. The review of this article was arranged by Editor C. Surya. *(Corresponding authors: Jigang Hu; Linbao Luo.)*

Li Wang, Hehao Luo, Huanhuan Zuo, Jiqing Tao, Yongqiang Yu, Xiaoping Yang, Molin Wang, Jigang Hu, Chao Xie, and Linbao Luo are with the School of Electrical Science and Engineering, Hefei University of Technology, Hefei 230009, China (e-mail: hujigang@hfut.edu.cn; luolb@hfut.edu.cn).

Di Wu is with the School of Physics and Microelectronics, Zhengzhou University, Zhengzhou 450052, China.

Color versions of one or more of the figures in this article are available online at http://ieeexplore.ieee.org.

Digital Object Identifier 10.1109/TED.2020.3001245

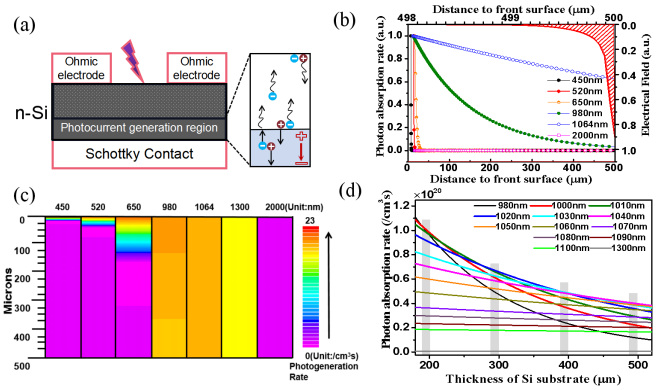

Fig. 1. (a) Schematic of the narrowband photodetector based on Si Schottky-junction. Simulated (b) electrical field and normalized photon absorption rate versus distance to front surface. (c) Contour maps photo-generation rate as a function of incident light wavelength and depth in Si. (d) Photon absorption rate of 980–1300-nm light in different thickness Si substrate.

by pasting In–Ga alloy onto the unpolished surface, enhancing the recombination on the incidence plane.

B. Device Characterization

The electrical measurement was performed on a semiconductor parameter testing system (Keithley 2400), and spectral response was measured on a monochrometer (LE-SP-M300). To study the photoresponse, laser diodes with different wavelengths (HW520AL35-16GD, FU650AD5-BC9, FU980AD100BD10, ZLM50AD1064-22130BXS, M265L3, M450LP1, M1550L3, M1650L4, and M1300L3) were used as light sources. The power intensity of all light sources was carefully calibrated using a power meter (Thorlabs GmbH., PM 100D) before measurement. All studies were conducted under ambient conditions at room temperature.

C. Numerical and Simulation

Simulation was carried out using Synopsys Sentaurus TCAD to analyze the photogeneration rate, photon absorption rate, and electric field in the device. A 2-D structure was constructed as shown in Fig. 1(a), with the dimension of 10 μm $\times$ 500 μm, consisting of a 500 μm-thick n-type phosphorous-doped (100) Si substrate (5×10^{14} cm^{-3}). The lengths of Ohmic and Schottky electrodes were set to be 1 and 10 μm, respectively. Grid points number of $\sim$31 810 was chosen as a compromise between computing time and precision, since finer meshes have been tried without obvious changes observed. A beam of light was introduced to the front surface of the Si substrate at an incident angle of 90°. Moreover, Shockley–Read–Hall statistics was adopted for the generation-recombination processes modeling.

III. Results and Disscusion

A schematic of the device is presented in Fig. 1(a). As well documented in other conventional device, only photo-generated free electron hole pairs (EHPs) in the specific area next to the Schottky contact can be collected by electrodes. This area is termed as photo-current generation region, which contains diffusion and depletion regions. The upper right red shaded area in Fig. 1(b) exhibits the simulated electric field in the depletion region of a device with 500 μm Si substrate. The electric field is located in a $\sim$2 μm wide region with intensity increasing significantly near the Schottky contact. Although the depletion region is much thinner than that of the diffusion region ($\sim$100 μm) [18], it, however, enables the efficient separation of EHPs to form photo-current. The spectral selectivity of the device should be mainly determined by the wavelength and corresponding quantity of photons absorbed by this narrow area. From Fig. 1(b), one can also learn that photon absorption rate declines sharply versus depth when the light wavelength deceases. This means the incident light with short wavelength can hardly enter into the deep region of silicon. Therefore, light illumination of wavelength less than 650 nm can hardly cause the formation of EHPs, when the depth in Si is larger than 150 μm [see Fig. 1(c)]. On the contrary, the light illumination at 1060 nm wavelength can generate EHPs at almost the whole depth of Si. Meanwhile there is little photogeneration, which reduces gradually to zero with the increase of wavelength, considering the lower irradiation energy than the Si bandgap. These calculation results indicate that selective spectral detection can be easily achieved by changing Si substrate thickness based on the simple device structure represented in Fig. 1(a).

The photoresponse of device was then explored by plotting the simulated curves of photon absorption rate with Si substrate thickness in the wavelength range of 980–1300 nm [see Fig. 1(d)]. Although the photon absorption rate of shorter wavelength is higher than that of the longer one, the absorption in Si at deeper depth however is dominated by longer wavelength light because of its slower attenuation trend of photon absorption. The gray pillars in Fig. 1(d) represent the position of the depletion region in Si substrate of different thicknesses. It is apparent that both the response peak and full width at half maximum (FWHM) can be controlled by Si wafer thickness, even when considering the contribution of diffusion region.

To verify the rationale outlined above, the I–V curves of the device based on n-silicon (500 μm)/Au Schottky-junction were measured in darkness and under illumination of different wavelengths at the same intensity [see Fig. 2(a)]. The device exhibited pronounced response to the 1064 nm illumination, while the photoresponse to other wavelengths were substantially tempered. Specifically, except for 1064 and 980 nm, the curves measured under light illumination of other wavelengths can hardly be distinguished with that measured in dark. Although this photoelectric effect is weak, it, however, can allow the device to operate under zero bias [inset in Fig. 2(a)]. In order to shed light on how the work function of electrode will affect the photoresponse performance, other electrode materials such as Al (4.1 eV), Ag (4.3 eV) and graphene (4.5 eV) were also employed to construct Schottky junction with n-Si for comparison [19]. From the inset in Fig. 2(b), one can find that photocurrents of these devices went up in an interesting order which is correlated with the work function value of their Schottky contact material. This finding is consistent with the simulation results shown in Fig. 2(b). Among the four devices composed of different Schotty junctions, the device with Au electrodes showed the largest photoresponse with steep rise and fall edges, signifying fast and effective separation of EHPs by the strong electric field in the depletion region. In light of this, Au electrodes were used for assembling the Schottky contact in the following discussion.

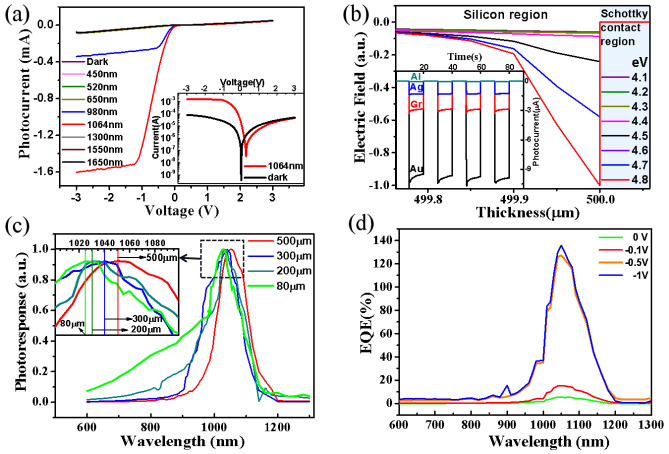

Fig. 2. (a) *I–V* curves of the photodetector based on Si/Au Schottky-junction under the illumination of different wavelength (3.5 mw/cm^2). The inset shows the photovoltaic behavior in semilogarithmic scale. (b) Time-dependent photoresponses and simulated electric field of the devices with different Schottky contacts. (c) Normalized wavelength-dependent photoresponse of the devices with the Si substrate of different thicknesses. (d) Wavelength-dependent EQEs under various bias voltages (275 μw/cm^2).

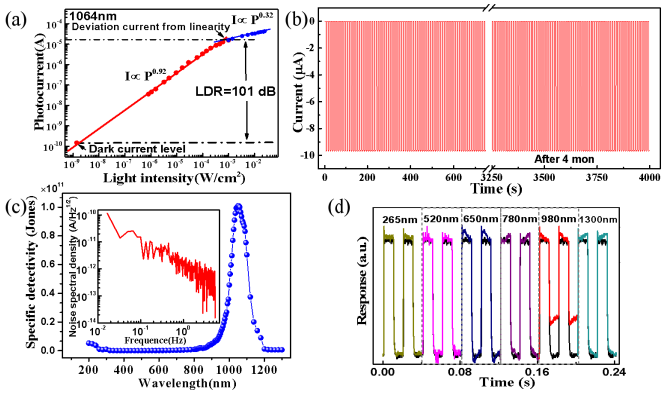

Fig. 3. (a) LDR measured at 0 V (pump wavelength 1064 nm). (b) Time-dependent photoresponse for about 75 cycles of operation at zero bias before and after four months storage under ambient condition. (c) Detectivity as a function of wavelength under illumination with an intensity of 3.35 μW/cm^2 at zero bias, and inset is the corresponding noise spectral density. (d) Time–response of the device to the signal of 1064 nm under background disturbance of other wavelength light.

Further experimental results showed that all Si devices with thicknesses of 80, 200, 300, and 500 μm exhibited obvious spectral selectivity [see Fig. 2(c)], however, their corresponding FWHMs were found to increase slightly from 107 to 175 nm as the Si thickness decreased from 500 to 80 μm. Meanwhile, the peak response slightly blue shifts from 1050 to 1025 nm. This phenomenon coincides well with the theory interpreted above. The increase of FWHM should be due to the arrival of more short-wavelength photons at the photocurrent generation region as the Si substrate thickness reduces. In addition to Si thickness, the bias voltage can also influence the photoresponse of narrowband device. For instance, the external quantum efficiency (EQE) of a 500 μm Si device can be improved to 135% at -1 V [see Fig. 2(d)], which is 24 times larger than that at 0 V. Since the EQE reflects the ratio of the number of charge carrier circulating in the circuit over the number of photons absorbed by device

$$\mathrm{EQE} = \left(I_{\mathrm{ph}}^{*}/e\right)/(PS/h\nu) \tag{1}$$

where I_{ph}^{*} is the net photocurrent, e is the electronic charge, P is the incident power density, S is the effective illumination area, h is the Plank's constant, and ν is the frequency of incident light [20]. The EQE value which is larger than 100% indicates that there should be a gain mechanism during the photodetection process. As shown in Fig. 1(a), the holes in the photocurrent generation region, especially in the depletion region, will be swept to the adjacent Schottky electrode, while the electrons need to pass through the entire n-type Si substrate to reach the Ohmic electrodes by diffusion. This will greatly prolong the carrier lifetime as the recombination ratio was lowered. Meanwhile, the difference between the transit times of electron and hole will increase with the increase of bias voltage, which would cause more external photo-current to maintain electric neutrality. Thereby, the gain effect became significant at negative bias. As a matter of fact, such a mechanism is similar to that of photoconductive detectors depending on the charge lifetime and the charge carrier transit time governed by the applied field [21]. Moreover, the FWHM and peak response were almost unchanged, which is probably due to the relative small change of depletion region width (<0.65 μm/V) caused by bias voltage (V) according to the formula

$$W_{\mathrm{dep}} = \sqrt{2\varepsilon_s(\psi_{bi} - V\text{-}k_0T/q)/qN_d} \tag{2}$$

where ε_s, ψ_{bi}, and N_d are, respectively, the permittivity of the semiconductor, the built-in potential, and the donor impurity concentration. The k_0T/q at room temperature is often neglected [22].

In addition, the linear dynamic range (LDR) of the device was calculated to be ~101 dB based on the light intensity-dependent photoresponse characteristics [see Fig. 3(a)], according to formula: LDR = $20\log(I_{\mathrm{ph}}^{*}/I_d)$, where I_d is the dark current [23]. LDR represents light intensity operating range of the device. The relative large LDR suggests that the recombination losses in the device are relatively low. This finding is further confirmed by the high value of corresponding θ, which is deduced to be 0.92 (close to the ideal value of 1) by fitting according to the power law: $I_{\mathrm{ph}}^{*} = P^{\theta}$ [24]. The low recombination losses should be the result of high crystalline quality of Si substrate and the majority carrier device nature of Schottky diode [25]. Moreover, the device exhibited excellent repeatability and long-term stability under continuously switched 1064 nm irradiation. The curve nearly kept unchanged even after four month storage in ambient condition [see Fig. 3(b)]. This excellent stability should be due to the superior stability of both Au and Si substrate. What is more, the specific detectivity (D^*) of the device was calculated to evaluate its ability of detecting weak optical signal

$$D^{*} = (S\Delta f)^{1/2}/\mathrm{NEP} \tag{3}$$

$$NEP = \bar{i}_n^{1/2}/R \tag{4}$$

$$R = I_{\mathrm{ph}}^{*}/(P \cdot S) \tag{5}$$

where Δf, NEP, R, and $\bar{i}_n^{1/2}$ denote bandwidth, noise equivalent power, responsivity, and the root-mean-square value of noise current, respectively, [23], [26]. As presented

in the inset of Fig. 3(c), the noise level per unit bandwidth was deduced to be 9.64×10^{-13} $\mathrm{AHz}^{-1/2}$ by performing a Fourier transformation of the dark current. The peak specific detectivity at 1050 nm, therefore, was estimated to be about 1.01×10^{11} Jones under 0 V, which is comparable to commercial PbS detector (Thorlabs, FDPS3X3, 1×10^{11} Jones). Considering the very weak absorption coefficient of Si at around 1060 nm, the relatively high D^* should be correlated with the gain effect mentioned above. Finally, to explore the anti-interference capability of the present narrowband device, additional light of other six different wavelengths such as 265, 520, 650, 780, 980, and 1300 nm with the same intensity was intentionally illuminated onto the photodetector which has been already shined by 1064 nm light (1 mW/cm^2). It can be easily seen from Fig. 3(d) that except the 980 nm, the photoresponse under other optical interference with wavelengths in the region from UV to visible and infrared are nearly the same, implying its excellent anti-interference capability to background disturbance.

IV. Conclusion

In summary, we have successfully developed a self-powered narrowband photodetector with a peak response near 1060 nm based on a simple Si Schottky junction. The FWHM of the device decreases from 175 to 107 nm as the Si thickness increases from 80 to 500 μm. Meanwhile, the peak response slightly red shifts from 1025 to 1050 nm. The EQE of the device based on 500 μm Si can be improved to 135% at -1 V, which is 24 times larger than that at zero bias. Moreover, the device exhibited excellent repeatability and long-term stability due to the superior stability of both Au and Si substrate. Its peak specific detectivity at 1050 nm was estimated to be about 1.01×10^{11} Jones under 0 V, which is comparable to commercial PbS detector. Benefiting from the high crystalline quality of the Si substrate and the majority carrier device nature of the Schottky diode, the device also represented relative large LDR (~101 dB). The spectral selectivity of the device can greatly enhance the noise immunity of infrared system. Meanwhile these results provide the possibility for application of the Schottky junction in narrowband detection due to its self-powered work mode, simple structure, low cost, and high sensitivity.

References

[1] X. Guo *et al.*, "High-responsivity Si photodiodes at 1060 nm in standard CMOS technology," *IEEE Electron Device Lett.*, vol. 39, no. 2, pp. 228–231, Feb. 2018, doi: 10.1109/LED.2017.2787147.

[2] K. Li, C. Chase, P. F. Qiao, and C. J. Chang-Hasnain, "Widely tunable 1060-nm VCSEL with highcontrast grating mirror," *Opt. Express*, vol. 25, no. 10, pp. 11844–11854, May 2017, doi: 10.1109/LED.2017.2787147.

[3] M. McClish, R. Farrell, R. Myers, F. Olschner, G. Entine, and K. S. Shah, "Recent advances of planar silicon APD technology," *Nucl. Instrum. Methods Phys. Res. A, Accel. Spectrom. Detect. Assoc. Equip.*, vol. 567, no. 1, pp. 36–40, Nov. 2006, doi: 10.1016/j.nima.2006.05.055.

[4] A. Rogalski, *Infrared Detector*. Amsterdam, The Netherlands: Gordon and Breach Science Publishers, 2000, p. 32.

[5] R. D. Jansen-van Vuuren, A. Armin, A. K. Pandey, P. L. Burn, and P. Meredith, "Organic photodiodes: The future of full color detection and image sensing," *Adv. Mater.*, vol. 28, no. 24, pp. 4766–4802, Jun. 2016, doi: 10.1002/adma.201505405.

[6] S. Yokogawa, S. P. Burgos, and H. A. Atwater, "Plasmonic color filters for CMOS image sensor applications," *Nano Lett.*, vol. 12, no. 8, pp. 4349–4354, Aug. 2012, doi: 10.1021/nl302110z.

[7] H. S. Rao, W. G. Li, B. X. Chen, D. B. Kuang, and C. Y. Su, "*In situ* growth of 120 cm^2 $CH_3NH_3PbBr_3$ perovskite crystal film on FTO glass for narrowband-photodetectors," *Adv. Mater.*, vol. 29, no. 16, 28220970, Apr. 2017, doi: 10.1002/adma.201602639.

[8] Q. Lin, A. Armin, P. L. Burn, and P. Meredith, "Filterless narrowband visible photodetectors," *Nature Photon.*, vol. 9, no. 10, pp. 687–694, Oct. 2015, doi: 10.1038/nphoton.2015.175.

[9] A. Solanki, S. Li, H. Park, and K. B. Crozier, "Harnessing the interplay between photonic resonances and carrier extraction for narrowband germanium nanowire photodetectors spanning the visible to infrared," *ACS Photon.*, vol. 5, no. 2, pp. 520–527, Nov. 2017, doi: 10.1021/acsphotonics.7b01034.

[10] K. B. Crozier, K. Seo, H. Park, A. Solanki, and S.-Q. Li, "Controlling the light absorption in a photodetector via nanowire waveguide resonances for multispectral and color imaging," *IEEE J. Sel. Topics Quantum Electron.*, vol. 24, no. 6, pp. 1–12, Nov. 2018, doi: 10.1109/JSTQE.2018.2840342.

[11] Q. Xiong, F. I. Chowdhury, and X. Wang, "Filter-free narrowband photodetectors employing colloidal quantum dots," *IEEE J. Sel. Topics Quantum Electron.*, vol. 24, no. 2, pp. 1–6, Mar. 2018, doi: 10.1109/JSTQE.2017.2776522.

[12] J. Li *et al.*, "Self-trapped state enabled filterless narrowband photodetections in 2D layered perovskite single crystals," *Nature Commun.*, vol. 10, no. 1, p. 806, Feb. 2019, doi: 10.1038/s41467-019-08768-z.

[13] Y. Zhao *et al.*, "High-electron-mobility and air-stable 2D layered $PtSe_2$FETs," *Adv. Mater.*, vol. 29, no. 5, Feb. 2017, Art. no. 1604230, doi: 10.1002/adma.201604230.

[14] Y. Zhao *et al.*, "Extraordinarily strong interlayer interaction in 2D layered PtS_2," *Adv. Mater.*, vol. 28, no. 12, pp. 2399–2407, Mar. 2016, doi: 10.1002/adma.201504572.

[15] M. Tanzid *et al.*, "Combining plasmonic hot carrier generation with free carrier absorption for high-performance near-infrared silicon-based photodetection," *ACS Photon.*, vol. 5, no. 9, pp. 3472–3477, Aug. 2018, doi: 10.1021/acsphotonics.8b00623.

[16] A. Sobhani *et al.*, "Narrowband photodetection in the near-infrared with a plasmon-induced hot electron device," *Nature Commun.*, vol. 4, no. 1, p. 1643, Mar. 2013, doi: 10.1038/ncomms2642.

[17] D. Periyanagounder *et al.*, "Fast-response, highly air-stable, and water-resistant organic photodetectors based on a single-crystal Pt complex," *Adv. Mater.*, vol. 32, no. 2, Jan. 2020, Art. no. 1904634, doi: 10.1002/adma.201904634.

[18] M. E. Law, E. Solley, M. Liang, and D. E. Burk, "Self-consistent model of minority-carrier lifetime, diffusion length, and mobility," *IEEE Electron Device Lett.*, vol. 12, no. 8, pp. 401–403, Aug. 1991, doi: 10.1109/55.119145.

[19] G. Giovannetti, P. A. Khomyakov, G. Brocks, V. M. Karpan, J. van den Brink, and P. J. Kelly, "Doping graphene with metal contacts," *Phys. Rev. Lett.*, vol. 101, no. 2, Jul. 2008, Art. no. 026803, doi: 10.1103/PhysRevLett.101.026803.

[20] F. P. G. de Arquer, A. Armin, P. Meredith, and E. H. Sargent, "Solution-processed semiconductors for next-generation photodetectors," *Nature Rev. Mater.*, vol. 2, no. 3, p. 16100, Mar. 2017, doi: 10.1038/natrevmats.2016.100.

[21] M. I. Saidaminov *et al.*, "Planar-integrated single-crystalline perovskite photodetectors," *Nature Commun.*, vol. 6, no. 1, p. 8724, Nov. 2015, doi: 10.1038/ncomms9724.

[22] S. M. Sze and K. K. Ng, *Physics of Semiconductor Devices*. Hoboken, NJ, USA: Wiley, 2006, p. 137.

[23] X. Liu, L. Gu, Q. Zhang, J. Wu, Y. Long, and Z. Fan, "All-printable band-edge modulated ZnO nanowire photodetectors with ultra-high detectivity," *Nature Commun.*, vol. 5, no. 1, p. 4007, Jun. 2014, doi: 10.1038/ncomms5007.

[24] Z. Shao *et al.*, "Memory phototransistors based on exponential-association photoelectric conversion law," *Nature Commun.*, vol. 10, no. 1, Mar. 2019, Art. no. 1294, doi: 10.1038/s41467-019-09206-w.

[25] M. Trivedi and K. Shenai, "Power semiconductor devices," in *The Electrical Engineering Handbook*, vol. 2, W. K. Chen, Ed. San Diego, CA, USA, 2000, p. 163.

[26] Y. Yu *et al.*, "Graphene/MoS_2/Si nanowires Schottky-NP bipolar van der Waals heterojunction for ultrafast photodetectors," *IEEE Electron Device Lett.*, vol. 39, no. 11, pp. 1688–1691, Nov. 2018, doi: 10.1109/LED.2018.2872107.